Journal of Modern Technology
https://journal.krrishpub.com/index.php/jmt/index

RESEARCH ARTICLE

MPPT For Hybrid Energy System Using Machine Learning Techniques

Aman Vaijnath Solanke[a,*], Suman Kumar Verma[a], Satyam Kumar[a], Benneth Oyinna [b], Kenneth E. Okedu [c]

[a] *Department of Electrical Engineering, National Institute of Technology Andhra Pradesh, Tadepalligudem, Andhra Pradesh 534 101, India.*
[b] *Energy Access and Renewable Energy, Offshore Technology Institute, University of Port Harcourt, 5323, Choba, Rivers State, Nigeria.*
[c] *School of Information Technology and Engineering, Melbourne Institute of Technology, 3000, Melbourne, Victoria, Australia.*

Abstract

The share of renewable energy sources (RES) in the total energy production has been growing rapidly. With the improvement in photovoltaic panel design and manufacturing techniques the per unit cost of photovoltaic systems (PVS) generated electricity has dropped considerably. Wind Energy Conversion Systems (WECS) have also seen a steady drop in the per unit electricity generation cost. This along with the environmental benefits of RES has made them a promising technology for power generation soon. To maximize the energy yield we need to operate the PVS and WECS at the maximum power point (MPP). This ensures that at any given moment we extract the maximum possible power from the systems. The PVS and WECS can be combined together to reduce the uncertainty around the availability of any given natural resource (solar or wind) at the given time. This Hybrid System can produce more power per square meter of land and is more reliable than the separate PVS or WECS. In this paper we discuss a machine learning (ML) based approach for faster maximum power point tracking (MPPT) of a hybrid energy system (HES) and its comparison with the conventional Perturb and Observe(P&O) method.

Keywords: Hybrid Energy System, MPPT, Machine Learning, Artificial Neural Network.

Article information:
Published by: **Krrish Scientific Publications Pvt. Ltd.**
DOI: https://doi.org/10.71426/jmt.v1.i1.pp19-37
Received: *12 May 2024* | Revised: *06 Jun. 2024* | Accepted: *12 Jun. 2024* | Published: *08 Sep. 2024*

1. Introduction

A hybrid energy system consists of two or more power generation sources [1]- [4], [18]- [19]. For the sake of this paper, we have considered a hybrid system made of PVS and WECS. It is known that the RES suffer from the problem of the unpredictable nature of the availability of solar or wind power. Combining these systems together reduces our exposure to only one kind of energy resource thus ensuring more reliable power supply at any given time [5]- [10].

Continuous tracking of the MPP is important to extract the maximum possible power from the system. Traditional algorithms like P&O, Incremental Conductance (InC), etc. [3] for PV and Tip Speed Ratio (TSR),

*Corresponding author
Email addresses: amansolanke007@gmail.com, 520238@student.nitandhra.ac.in (Aman Vaijnath Solanke), krsk1495@gmail.com, 520241@student.nitandhra.ac.in (Suman Kumar Verma), satyamvisa3005@gmail.com, 520235@student.nitandhra.ac.in (Satyam Kumar), benneth.oyinna@nesconigeria.com, bennethoyinna@gmail.com (Benneth Oyinna), kenokedu@mit.edu, kokedu@academic.mit.edu.au (kenneth E. Okedu).

Hill Climbing, etc. [4] for WECS take time to converge. By the time the algorithm converges, the MPP shifts to a new location, thus, operating at the MPP for a longer time becomes difficult.

We used machine learning to provide a starting point for the widely used P&O algorithm to considerably increase its speed for the real-time tracking of the MPP [14]. By reducing the number of iterations, it takes for the P&O algorithm to converge will allow us to operate at the MPP for longer durations and improve the energy efficiency of the system. Artificial Neural Networks (ANN) were trained to predict the MPP voltage and power for the WECS and PVS. The expected duty ratios for the boost converters connected to the WECS and PVS were calculated based on the output of the respective ANNs. This duty ratio was used as a starting point for the P&O to search for the MPP.

2. Mathematical modeling of a PV system [5], [6]

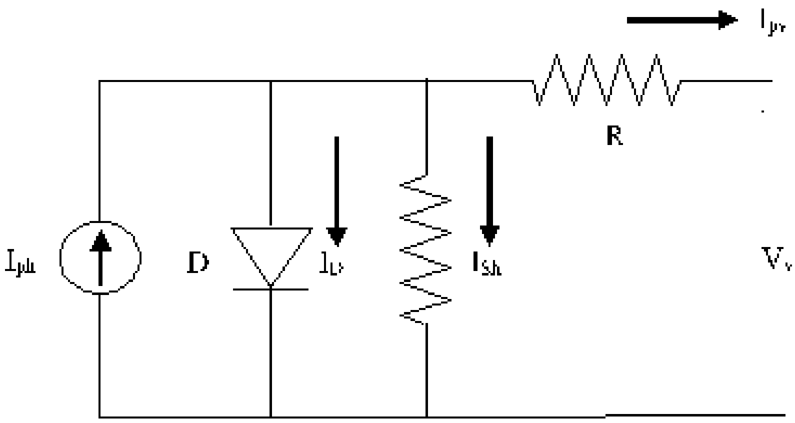

Figure 1: Circuit diagram of a PV cell.

The PV current is given by the below equation Figure 1,

$$I_{pv} = I_{ph} - I_D - I_{sh} \tag{1}$$

Photovoltaic current can be calculated as follows,

$$I_{phn} = I_{scn} \tag{2}$$

$$I_{ph} = (I_{phn} - K_i (T - T_n)) \left(\frac{G}{G_n} \right) \tag{3}$$

Diode current can be calculated as follows Figure 2, Figure 3,

$$V_t = \frac{N_s k T}{q} \tag{4}$$

$$I_{on} = \frac{I_{scn}}{e^{\left(\frac{V_{ocn}}{a V_{tn}} - 1\right)}} \tag{5}$$

$$I_o = I_{on} \left(\frac{T}{T_n} \right)^3 e^{\left(\frac{q E_g}{a k}\right)\left(\frac{1}{T_n} - \frac{1}{T}\right)} \tag{6}$$

$$I_D = I_o e^{\left(\frac{V_{pv} + I_{pv} R_s}{\eta V_t} - 1\right)} \tag{7}$$

Current through the shunt branch can be calculated as follows,

$$I_{sh} = \frac{V_{pv} + I_{pv} R_s}{R_{sh}} \tag{8}$$

V_{tn}: Thermal voltage (V)
N_s: No of panels in series
k: Boltzmann's constant (J/K)
T_n: Reference temperature (K)
q: Electron charge (C)
I_{on}: Diode saturation current (A)
I_{scn}: Reverse bias saturation current (A)
V_{ocn}: Diode open-circuit voltage (V)
a: Diode ideality factor
I_o: Diode current (A)
T: Operating temperature (K)
E_g: Bandgap voltage of the semiconductor (eV)
I_{phn}: Photovoltaic current at reference temperature (A)
K_i: Photocurrent temperature coefficient (A/K)
G: Irradiance (W/m^2)
G_n: Reference irradiance (W/m^2)
V_t: Thermal voltage at operating temperature (V)

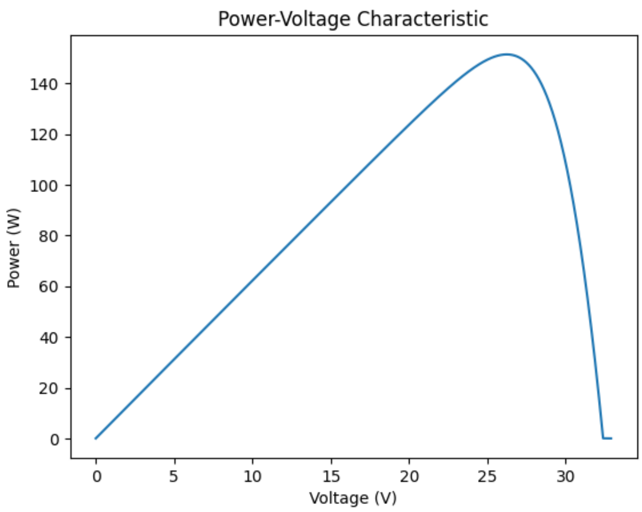

Figure 2: Power vs voltage characteristics of PV cell.

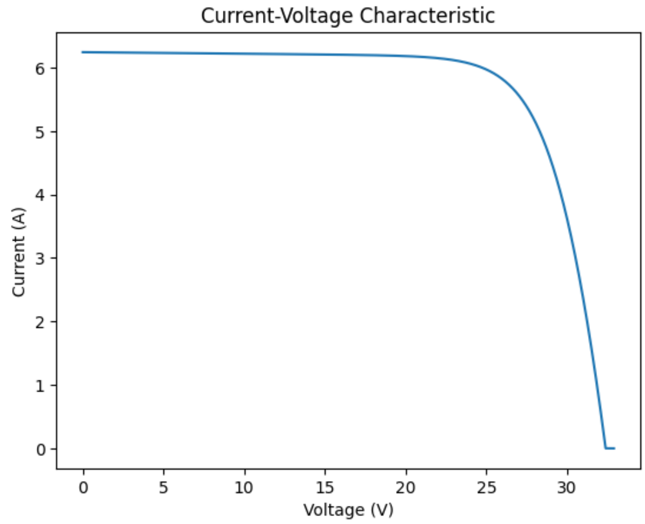

Figure 3: Current vs voltage characteristics of PV cell.

3. Mathematical modeling of a DC generator and a WECS [6]

We have used a separately excited DC generator to capture the power generated by the turbine [7]. This also ensures easy connection with the boost converter and eliminates the need for an intermediate rectifier Figure 4 and power vs turbine speed characteristics of a WECS Figure 5.

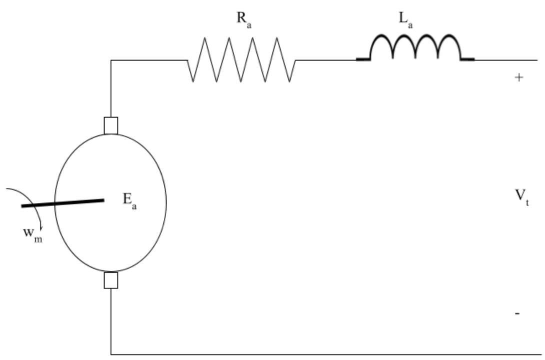

Figure 4: Circuit diagram of a DC generator.

$$V_t = E_a - I_a R_a - L_a \frac{dI_a}{dt} \tag{9}$$

$$E_a = k_1 \phi \omega_m \tag{10}$$

For negligible voltage drop in the armature winding it can be assumed that,

$$V_t \approx E_a \tag{11}$$

V_t: Voltage at the terminal (Volts)
E_a: Back EMF (Volts)
I_a: Armature current (A)
R_a: Armature resistance (Ω)
L_a: Armature Inductance (H)
K_1 is given by $\dfrac{\text{No. of Poles} \times \text{No. of Armature Conductors}}{2\pi \times \text{No. of Parallel Paths}}$
ϕ: Field flux ($\mathrm{Wb/m^2}$)
ω_m: Angular velocity of the rotor (rad/sec)

$$P_w = \frac{1}{2}\rho A v^3 \tag{12}$$

$$\lambda = \frac{\omega R}{v} \tag{13}$$

$$P = \frac{1}{2}C_p(\lambda, \beta)\rho A v^3 \tag{14}$$

$$C_p(\lambda, \beta) = 0.5176\left[\left(\frac{116}{\lambda_i} - 0.4\beta - 5\right)e^{-21/\lambda_i} + 0.0068\lambda_i\right] \tag{15}$$

$$\frac{1}{\lambda_i} = \frac{1}{\lambda + 0.08\beta} - \frac{0.035}{\beta^3 + 1} \tag{16}$$

ρ: Air density ($\mathrm{kg/m^3}$)
A: Swept area of the rotor blade ($\mathrm{m^2}$)
v: Wind velocity (m/s)
P: power captured by the wind turbine (W)
$C_p(\lambda, \beta)$: Power coefficient
λ: Tip speed ratio
β: Pitch angle (degrees)
ω: Turbine angular speed (rad/s)
R: Radius of the turbine (m).

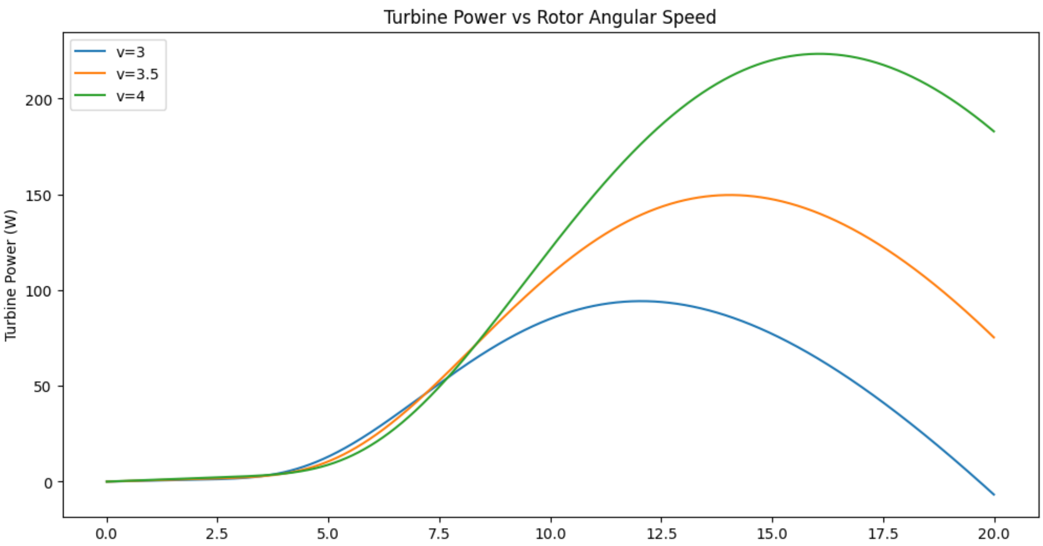

Figure 5: Power vs turbine speed characteristics of a WECS.

4. Boost converter

A boost converter is a power electronic device Figure 6. It increases the voltage at its output terminal with respect to the voltage at its input terminal by varying the duty ratio [8], [9]. By changing the duty ratio of the boost converter, we can change the load as perceived by the PVS or WECS and thus always operate at the MPP.

The output voltage of the boost converter and other modelling equations are given by the following equation (17)–(22).

$$V_o = \frac{V_{in}}{1-d} \tag{17}$$

Assuming negligible loss in the boost converter we can state that the input power will be equal to the output power.

Therefore,

$$V_{in}I_{in} = V_oI_o \tag{18}$$

$$I_o = I_{in}(1-d) \tag{19}$$

$$P_{in} = V_oI_o = \frac{V_o^2}{R_L} \tag{20}$$

Hence, from (18), (19) and (20)

$$P_{in} = \frac{V_{in}^2}{(1-d)^2 R_L} \tag{21}$$

From (21) the duty cycle can be given as,

$$d = 1 - \frac{V_{in}}{\sqrt{P_{in}R_L}} \tag{22}$$

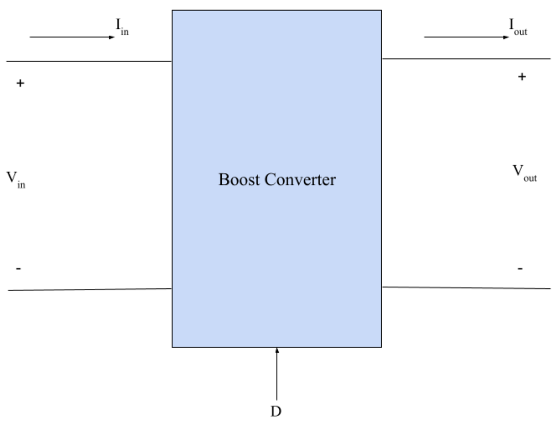

Figure 6: Boost converter.

In (17)–(22), the terms are:
V_o: Voltage at the output terminal (V)
I_o: Current at the output terminal (A)
V_{in}: Voltage at the input terminal (V)
I_{in}: Current at the input terminal (A)
d: Duty ratio
P_{in}: Power at the input terminal (Watts)
R_L: Load Resistance connected to the output terminal (Ω)

5. Artificial neural network

Machine Learning is a powerful tool. With the help of AI/ML several engineering problems can be solved faster than the conventional methods used by the industries. The ML models act as a support system to improve the efficiency of the conventional algorithms by adding an element of intelligence to the traditional algorithms.

Deep Learning (DL) is a subfield of ML and ANNs are the backbone of Deep Learning. A neural network comprises several layers divided into three categories, namely, Input Layer, Hidden Layers, and Output Layer. Each layer is made up of several neurons also called as perceptron. A neuron is inspired from the biological neurons present in the human brain. Thus, an ANN mimics the prediction and decision-making abilities of a human brain. A neuron can further be divided into three important components, the weights, the bias, and the activation function. During the training process we train the weights of the neurons to better predict the output [10].

Two separate neural networks were trained to predict the MPP voltage and power for both the PVS and WECS. The inputs provided for the ANN predicting the MPP voltage and power of the PV system were the solar irradiance(G) and the temperature(T). The input provided for the ANN predicting the MPP voltage and power for WECS is the wind speed (v). The output received from the ANNs, for both the systems, is the expected voltage(V) at the terminal at which the maximum power occurs and the expected magnitude of maximum power(P). The ANN for PVS Visualization is shown in Figure 7.

5.1. ANN for PVS

Number of Layers: 5 (3 Hidden Layers)
Layer 1: Input Layer; 2 Perceptrons
Layer 2: Hidden Layer; 100 Perceptrons; ReLU Activation
Layer 3: Hidden Layer; 100 Perceptrons; ReLU Activation
Layer 4: Hidden Layer; 100 Perceptrons; ReLU Activation
Layer 5: Output Layer; 2 Perceptrons; Linear Activation
Optimizer: Adam
Loss Function: Mean Absolute Error (MAE)
Epochs: 100
Batch Size: 50

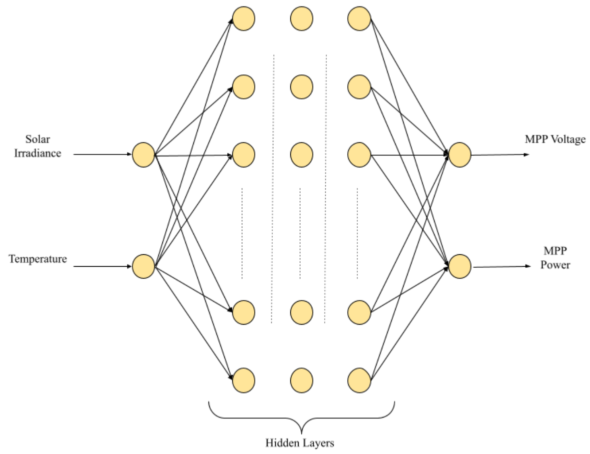

Figure 7: ANN for PVS visualization.

5.2. ANN for WECS

The ANN for WECS Visualization is shown in Figure 7 and Figure 8. The layer details are given bellow.
Number of Layers: 5 (2 Hidden Layers, 1 Dropout Layer)
Layer 1: Input Layer; 1 Perceptrons
Layer 2: Hidden Layer; 50 Perceptrons; ReLU Activation
Layer 3: Hidden Layer; 50 Perceptrons; ReLU Activation
Layer 4: Dropout Layer; 25% Dropout
Layer 5: Output Layer; 2 Perceptrons; Linear Activation
Optimizer: Adam
Loss Function: Mean Squared Error (MSE)
Epochs: 100
Batch Size: 50

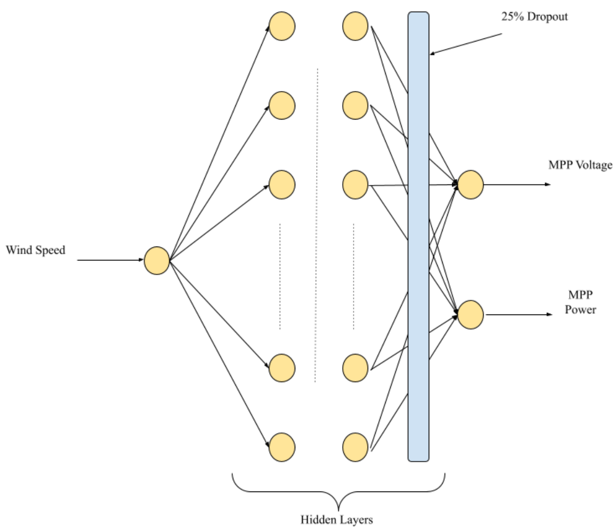

Figure 8: ANN for WECS visualization.

6. P&O Algorithm

Perturb and Observe algorithm, as the name suggests, varies the duty cycle by a small amount ΔD and measures the corresponding voltage (V_k) and power (P_k) at the output terminal of the PV panel or the DC generator. It compares these readings with the previous voltage (V_{k-1}) and power (P_{k-1}) and the duty ratio (D_k) is increased or decreased accordingly [11]–[12].

7. ANN + P&O Algorithm

In the case of conventional P&O algorithm the new MPP search starts from the previous duty ratio. Thus, the time taken for convergence is higher in cases of significant changes in the operating conditions. Also, this method is prone to converging at the local maxima in cases of partial shading in PVS.

The proposed ANN+P&O algorithm uses the prediction capability of the ANN to add an element of intelligence to the conventional P&O algorithm. The proposed algorithm thus starts the search for the MPP from the duty ratio predicted by the ANN which is expected to be closer to the global maxima. Thus, the number of iterations taken to arrive at the predicted point are saved and a direct jump close to the global maxima is obtained. This reduces the time for convergence. Block diagram of ANN + P&O is shown in Figure 10.

8. Comparision of ANN+P&O with conventional P&O

As discussed earlier, the starting point for the P&O is provided by the ANN. This ANN+P&O algorithm converges in fewer iterations as compared to the conventional P&O algorithm Figure 9.

To test the hypothesis an initial operating point of duty ratio 0.20 for PVS and 0.3647 for WECS is considered. First the operating conditions change to 30.29°Celsius, 692.09 W/m^2 and 5m/s wind speed (Operating Condition 1). The operating conditions then change to 24.93°Celsius, 760.78W/m^2 and 4m/s wind speed (Operating Condition 2). Under all the changing conditions both the algorithms are made to track the MPP and the performance in terms of number of iterations until convergence is noted in the table along with the details of the operating conditions. Table 1 indicates operating conditions for hypothesis testing Figure 9.

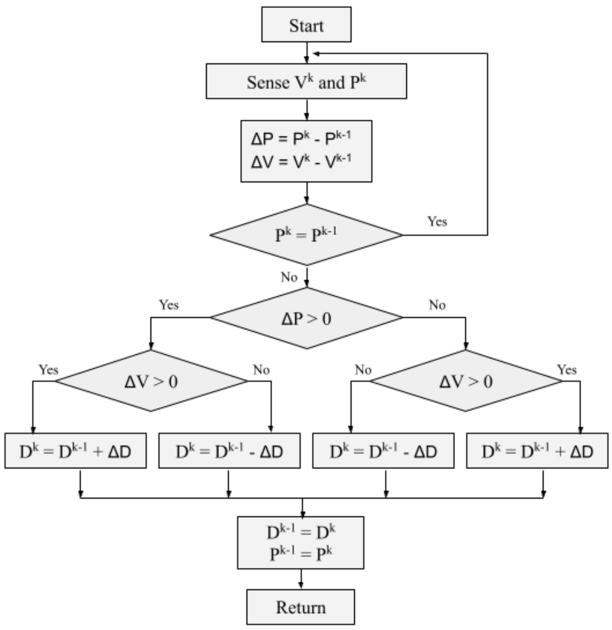

Figure 9: P&O Algorithm flowchart.

Table 1: Operating conditions for testing ANN+P&O algorithm.

	Temperature (°C)	Irradiance (W/m^2)	Wind Speed (m/s)
Initialization (Duty Ratio)	PVS: 0.20; WECS: 0.3647		
Operating Condition 1	30.29	692.09	5
Operating Condition 2	24.93	760.78	4

The Table 2 summarizes the changing conditions for PVS and compares the performance of Conventional P&O with the proposed ANN+P&O. The Table 3summarizes the changing conditions for WECS and compares the performance of Conventional P&O with the proposed ANN+P&O.

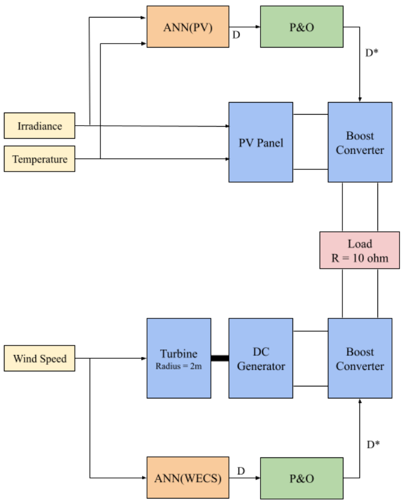

Figure 10: Block diagram of ANN + P&O.

Table 2: Performance comparison of conventional P&O with the proposed ANN+P&O for PVS.

T (°C)	G (W/m^2)	D_Previous for P&O	D_Predicted for ANN+P&O	D_ Actual	No. of Iterations until convergence for Conventional P&O	No. of Iterations until convergence for ANN+P&O
Initialization at previous duty ratio = 0.2						
30.29	692.09	0.2	0.2267	0.3015	1100	800
24.93	760.78	0.3015	0.3123	0.3253	250	130

Table 3: Performance of ANN+P&O for WECS.

v (m/s)	D_Previous for P&O	D_Predicted for ANN+P&O	D_Actual	No. of Iterations for Conventional P&O	No. of Iterations for ANN+P&O
Initialization at previous duty ratio = 0.3647 (v = 3m/s)					
5	0.3647	0.5852	0.5053	60	30
4	0.5053	0.4665	0.4496	50	10

The convergence graphs for both ANN+P&O and conventional P&O are shown Figure 11 along with the number of iterations required until convergence for operating condition 1. Comparing ANN+P&O with P&O for Operating Condition 1(WECS) is shown in Figure 12.

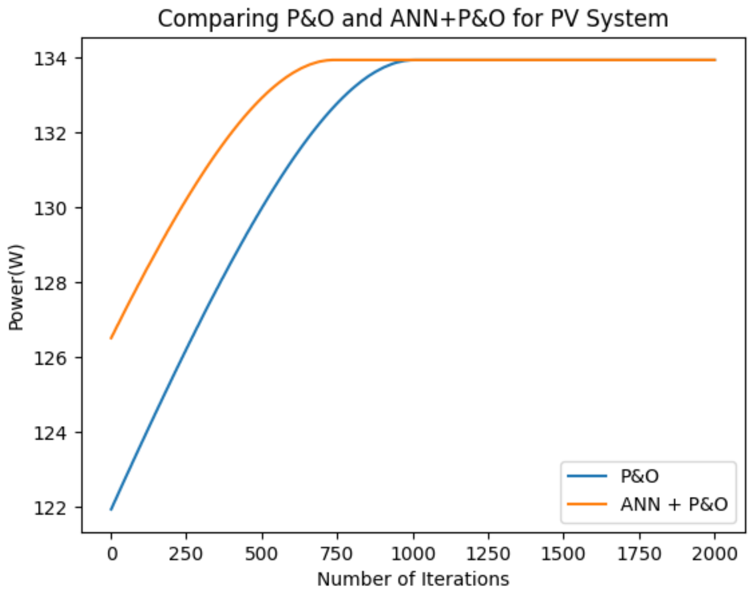

Figure 11: Comparing ANN+P&O with P&O for operating condition 1(PVS).

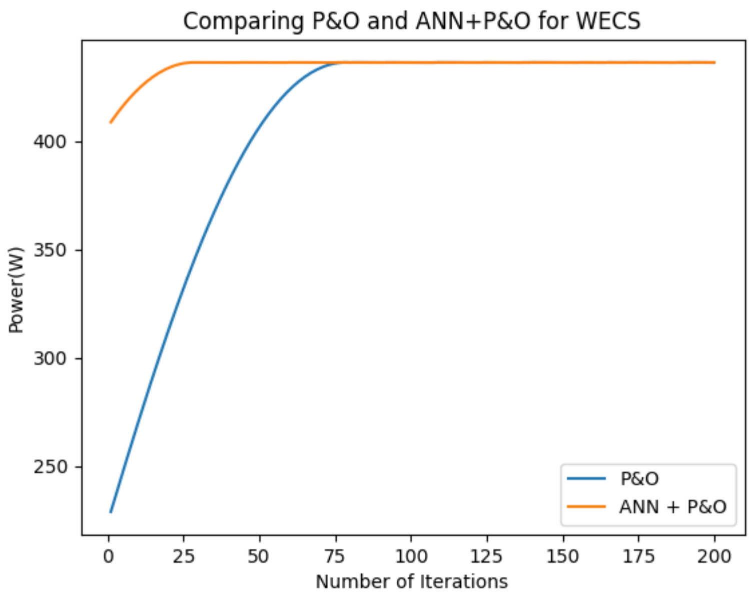

Figure 12: Comparing ANN+P&O with P&O for operating condition 1(WECS).

The convergence graphs for both ANN+P&O and conventional P&O are shown below along with the number of iterations required until convergence for operating condition 2 is shown in Figure 13.

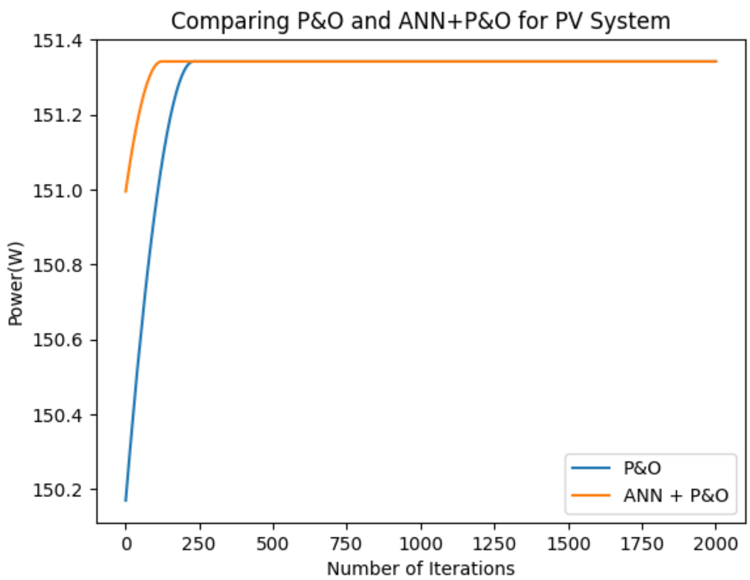

Figure 13: Comparing ANN+P&O with P&O for operating condition 2(PVS).

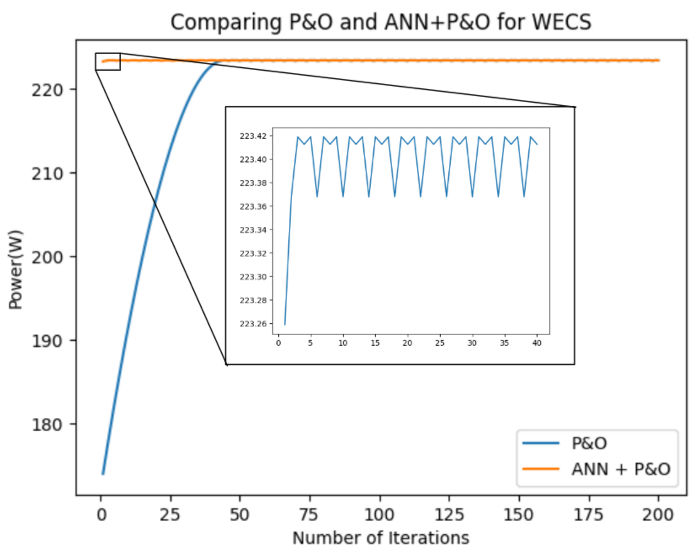

Figure 14: Comparing ANN+P&O with P&O for operating condition 2(WECS).

It can be seen that the ML powered P&O algorithm converges in fewer iterations as compared to the conventional P&O algorithm. In both cases the number of iterations required for the ANN+P&O algorithm are less than half of what the conventional algorithm requires. After the conditions changed the ANN+P&O algorithm jumped to the point closer to the MPP and then converged towards the MPP unlike the conventional P&O which continuously took small steps towards the MPP. Thus, saving time and maximizing the energy yield. The scatter plots those compare the predicted MPP with the actual MPP of PVS and WECS are shown in Figure 15 and Figure 16 respectively.

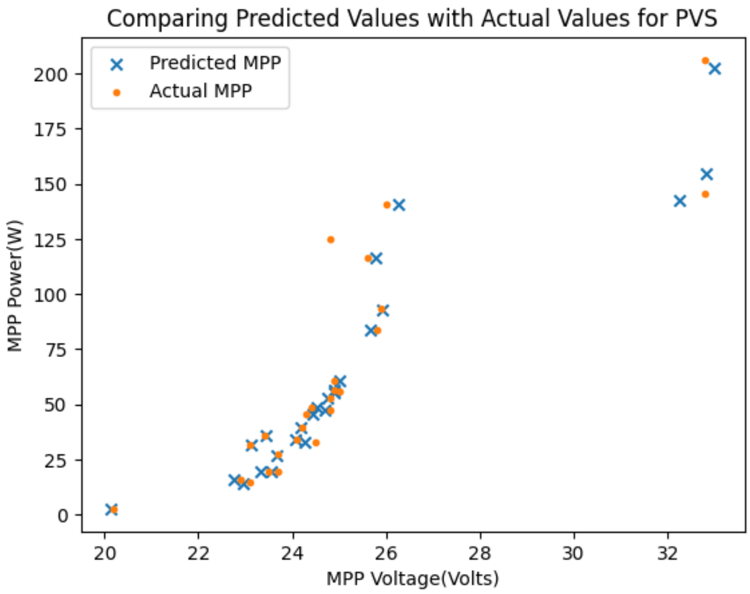

Figure 15: Predicted value vs actual values (PVS).

We can observe that the predicted MPP is very close to the actual MPP. Thus, giving the P&O algorithm a starting point which is very close to the actual MPP and speeding up the MPPT process.

9. Conclusion

In this paper, a ML powered P&O algorithm, ANN+P&O, was proposed. It was observed that the ML model added an element of intelligence to the conventional P&O algorithm by predicting the duty ratio for the current operating conditions. The conventional P&O algorithm then jumps to the predicted MPP point and starts converging. Without the ML model the P&O would have started looking for the new MPP from the previous MPP thus requiring more time, resulting in lower energy yield. The proposed algorithm converges in fewer iterations as compared to the traditional P&O and is therefore more reliable for real-time MPP tracking. This ensures higher energy yield and optimum use of the HES.

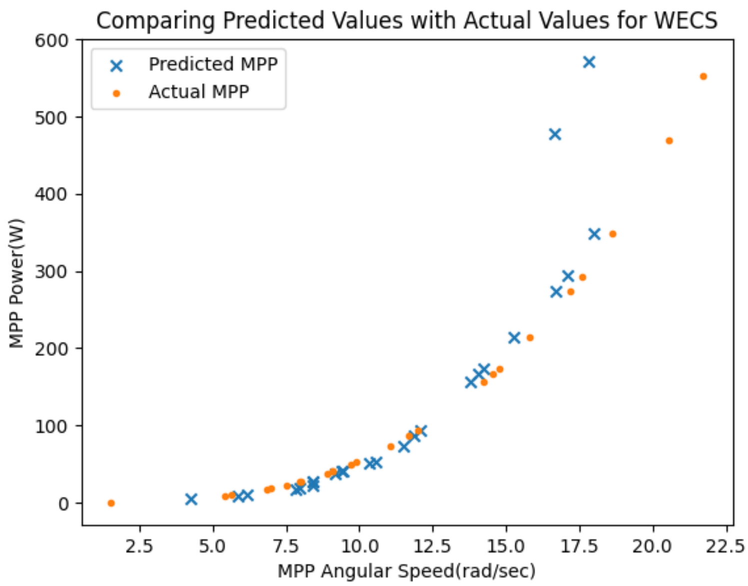

Figure 16: Predicted value vs actual values (WECS).

10. Psedo codes

The pseudo codes of the proposed work is given in the preceding subsections.

10.1. Calculating the IV characterstics of PVS:

PV Characteristic Equation(Calculating V and I)

$j \leftarrow 0;$
for $i \leftarrow 0$ to I_{sc} steps of 0.001 **do**
  $j \leftarrow 0;$
  $I_{pvc}(j,1) \leftarrow I;$
  $V_c(j,1) \leftarrow 0;$
  if $I < (I_{ph} - I_o)$ **then**
    $V_{pv}(j,1) = \left[V_{tcs} \cdot \log\left(\frac{I_{ph} - I - I_o}{I_o}\right) - IR_s\right] \cdot N_s;$
  else
    $V_{pv}(j,1) \leftarrow 0;$
  end if
  if $V_{pv}(j,1) < 0$ **then**
    $V_{pv}(j,1) \leftarrow 0;$
  end if
end for

10.2. Training ANN for predicting MPP for PVS:

Training ANN for PVS

Input: $Xpv_{train}, Ypv_{train}, Xpv_{test}, Ypv_{test}$ ▷ Training and testing data
Output: *model* ▷ Trained neural network model

```
model ← Sequential()
model.add(Dense(units=100, activation='relu', input_shape=[2]))
model.add(Dense(units=100, activation='relu'))
model.add(Dense(units=100, activation='relu'))
model.add(Dense(units=2, activation='linear'))
early_stopping ← EarlyStopping(min_delta=0.001,
        patience=15, restore_best_weights=True)
model.compile(optimizer='adam', loss='mae', metrics=['mse'])
history ← model.fit(Xpv_train, Ypv_train,
        validation_data = (Xpv_test, Ypv_test),
        batch_size = 50, epochs = 100, callbacks = [early_stopping])
```

10.3. Calculating power vs angular speed for WECS:

Wind Characteristic Equation (Calculating P and W)

function CALCULATE_LAMBDA(ω, R, v)
  return $\frac{\omega R}{v}$
end function
function INVERSE_LAMBDA_I(β, λ)
  return $\frac{1}{\lambda + 0.08\beta} - \frac{0.035}{\beta^3 + 1}$
end function
function $Cp(inverse\_lambda\_i, \lambda, \beta)$
  $term1 \leftarrow (116 \cdot inverse\_lambda\_i - 0.4 \cdot \beta - 5)$
    $\cdot \exp(-21 \cdot inverse\_lambda\_i)$

```
        term2 ← 0.0068 · λ
        return 0.5176 · (term1 + term2)
end function
function Calculate_Actual_Power(v, A, ρ, Cp, β)
        return 0.5 · ρ · A · v^3 · Cp
end function
beta_range ← [0, 2, 4, 6, 8, 10, 12, 14]                ▷ Range of beta values
v_values ← [3, 3.5, 4]                                  ▷ Wind speed values
for each β in beta_range do
        for each v in v_values do
                omega_vals ← [0, 0.01, 0.02, . . . , 24.99]     ▷ Range of omega values
                lambda_vals ← [calculate_lambda(ω, R, v) for ω in omega_vals]
                inverse_lambda_vals ← [inverse_lambda_i(β, λ) for λ in lambda_vals]
                Cp_vals ← [Cp(inv_lambda, λ, β) for inv_lambda, λ in zip(inverse_lambda_vals, lambda_vals)]
                actual_power_vals ← [calculate_actual_power(v, A, ρ, Cp, β) for Cp in Cp_vals]
                ▷ Plot omega_vals vs actual_power_vals for each v
        end for
end for
if Wind_speed is not NaN and is finite then
        omega_vals ← [1, 1.01, 1.02, . . . , 24.99]             ▷ Range of omega values
        lambda_vals ← [calculate_lambda(ω, R, Wind_speed) for ω in omega_vals]
        inverse_lambda_vals ← [inverse_lambda_i(β, λ) for λ in lambda_vals]
        Cp_vals ← [Cp(inverse_lambda, λ, β) for inverse_lambda, λ in zip(inverse_lambda_vals, lambda_vals)]
        actual_power_vals ← [calculate_actual_power(Wind_speed, A, ρ, Cp, β) for Cp in Cp_vals]
        if actual_power_vals is not empty then
                max_power_index ← index of max(actual_power_vals)
                Pmax ← actual_power_vals[max_power_index]
                omega_for_Pmax ← omega_vals[max_power_index]
        else
                Pmax ← 0
                omega_for_Pmax ← 0
        end if
else
        Pmax ← 0
        omega_for_Pmax ← 0
end if
```

10.4 Training ANN for predicting MPP for WECS:

Training ANN for WECS

```
Input: Xwind_train, Ywind_train, Xwind_test, Ywind_test        ▷ Training and testing data
Output: modelwind                                              ▷ Trained wind model
modelwind ← Sequential()
modelwind.add(Dense(units=50, activation='relu', input_shape=[1]))
modelwind.add(Dense(units=50, activation='relu'))
modelwind.add(Dropout(0.25))
modelwind.add(Dense(units=2, activation='linear'))
modelwind.compile(optimizer='adam', loss='mse', metrics=['mse'])
early_stopping ← EarlyStopping(min_delta=0.001,
        patience=15, restore_best_weights=True)
history ← modelwind.fit(Xwind_train, Ywind_train,
        validation_data = (Xwind_test, Ywind_test),
```

```
            batch_size = 50, epochs = 100, callbacks = [early_stopping])
```

10.5. P&O for PVS:

P&O for PV

```
function PANDOPV(dprev, iter_max)
    iter ← iter_max, deld ← 0.0001
    ind ← index of the min abs difference between dpv and dprev
    P_prev ← V[ind] × I[ind], V_prev ← V[ind]
    d ← dprev + 0.001
    Create arrays P_array and count_array of size max_iter, initialized with zeros
    count ← 0
    for i ← 0 to iter do
        count ← count + 1,
        index ← index of the min abs difference between dpv and d
        P_new ← V[index] × I[index], V_new ← V[index]
        delP ← P_new − P_prev, delV ← V_new − V_prev
        if delP ≠ 0 then
            if delP > 0 then
                if delV > 0 then
                    d ← d − deld
                else
                    d ← d + deld
                end if
            else
                if delV > 0 then
                    d ← d + deld
                else
                    d ← d − deld
                end if
            end if
        else
            d ← dprev
        end if
        dprev ← d, P_prev ← P_new, V_prev ← V_new
        Store P_new in P_array at index i, Store count in count_array at index i
    end for
    return P_array, count_array, d
end function
```

10.5. P&O for WECS:

P&O for WIND

```
function PANDOWIND(wprev, iter_max)
    iter ← iter_max
    delw ← 0.1
    ind ← index of the minimum absolute difference between omega_vals and wprev
    Pprev ← actual_power_vals[ind]
    Omegaprev ← omega_vals[ind]
    w ← wprev + 0.3
    Create arrays Parray and countarray of size iter, initialized with zeros
    count ← 0
```

```
    for i ← 0 to iter − 1 do
        count ← count + 1
        index ← index of the minimum absolute difference between omega_vals and w
        Pnew ← actual_power_vals[index]
        omeganew ← omega_vals[index]
        delP ← Pnew − Pprev
        delomega ← omeganew − Omegaprev
        if delP ≠ 0 then
            if delP > 0 then
                if delomega > 0 then
                    w ← w + delw
                else
                    w ← w − delw
                end if
            else
                if delomega > 0 then
                    w ← w − delw
                else
                    w ← w + delw
                end if
            end if
        else
            w ← Omegaprev
        end if
        Pprev ← Pnew
        Omegaprev ← omeganew
        Store Pnew in Parray at index i
        Store count in countarray at index i
    end for
    return Parray, countarray, w
end function
```

Declarations and ethical statements

Conflict of interest: The authors declare that there is no conflict of interest.
Funding statement: This research received no external funding.
Artificial Intelligence usage statement: During the preparation of this manuscript, the authors utilized ChatGPT solely for language refinement and grammatical corrections. The authors carefully reviewed and revised the generated content and take full responsibility for the accuracy, integrity, and originality of the final manuscript.
Availability of data and materials: The data and/or materials that support the findings of this study are available from the corresponding author upon reasonable request.
Acknowledgments: The authors, Mr. Aman, Mr. Suman and Mr. Satyam of this article would like to thank Dr. V. B Murali Krishna, a faculty member of department of Electrical Engineering, National Institute of Technology Andhra Pradesh for his valuable suggestions and guidance for completing this work.

CRediT authorship contribution statement

Aman Vaijnath Solanke: Conceptualization, Data curation, Methodology, Software, Investigation, Visualization, Writing–Original draft, Review & Editing. **Suman Kumar Verma**: Conceptualization, Methodology, Writing–Review & Editing. **Satyam Kumar**: Data curation, Formal analysis, Validation, Visualization, Writing–Review & Editing. **Benneth Oyinna** : Formal analysis, Writing–Review & Editing. **Kenneth E. Okedu**: Methodology, Validation, Formal analysis.

Publisher's note

Krrish Scientific Publications Pvt. Ltd. and the ***Journal of Modern Technology*** remain neutral with regard to jurisdictional claims in published maps and institutional affiliations.

References

[1] Elavarasan RM, Shafiullah GM, Padmanaban S, Kumar NM, Annam A, Vetrichelvan AM, Mihet-Popa L, Holm-Nielsen JB. A Comprehensive Review on Renewable Energy Development, Challenges, and Policies of Leading Indian States With an International Perspective. *IEEE Access*. 2020 Apr 20;8:74432-57. Available from: https://doi.org/10.1109/ACCESS.2020.2988011

[2] Kurbatova T, Perederii T. Global trends in renewable energy development. In *Proceedings of the 2020 IEEE KhPI Week on Advanced Technology (KhPIWeek)*. Kharkiv, Ukraine: IEEE; 2020. p. 260–263. Available from: https://doi.org/10.1109/KhPIWeek51551.2020.9250098

[3] Singh O, Gupta SK. A review on recent Mppt techniques for photovoltaic system. In *Proceedings of the 2018 IEEMA Engineer Infinite Conference (eTechNxT)*. New Delhi, India: IEEE; 2018. p. 1–6. Available from: https://doi.org/10.1109/ETECHNXT.2018.8385315

[4] Kumar D, Chatterjee K. A review of conventional and advanced MPPT algorithms for wind energy systems. *Renewable and Sustainable Energy Reviews*. 2016;55:957–970.

[5] Singh O, Rajput SK. Mathematical modelling and simulation of solar photovoltaic array system. In: *Proceedings of the 2016 International Conference on Research Advances in Integrated Navigation Systems (RAINS)*. IEEE; 2016. p. 1–5. Available from: https://doi.org/10.1109/RAINS.2016.7764395

[6] Kiran KB, Indira MS, Nagaraja R. Mathematical modeling and evaluation of performance characteristics of a hybrid solar PV and wind energy system. *Journal of Applied Science and Engineering*. 2021 Dec;25(4):785-97. Available from: https://doi.org/10.6180/jase.202208_25(4).0014

[7] Ma H, Chen L, Ju P, Liu H, Jiang N, Wang C. Feasibility research on DC generator based wind power generation system. In: *Proceedings of the 2009 International Conference on Sustainable Power Generation and Supply*. IEEE; 2009. p. 1–5. Available from: https://doi.org/10.1109/SUPERGEN.2009.5348170

[8] Fathah A. *Design of a Boost Converter* [dissertation]. 2013. online Available from: https://d1wqtxts1xzle7.cloudfront.net/95069605/109EE0612-libre.pdf

[9] Hasaneen BM, Mohammed AA. Design and simulation of DC/DC boost converter. In: *Proceedings of the 2008 12th International Middle-East Power System Conference*. IEEE; 2008. p. 335–340. Available from: https://doi.org/10.1109/MEPCON.2008.4562340

[10] Dongare AD, Kharde RR, Kachare AD. Introduction to artificial neural network. *International Journal of Engineering and Innovative Technology (IJEIT)*. 2012 Jul;2(1):189-194.

[11] Elgendy MA, Zahawi B, Atkinson DJ. Evaluation of perturb and observe MPPT algorithm implementation techniques. In: *Proceedings of the 6th IET International Conference on Power Electronics, Machines and Drives (PEMD 2012)*. IET; 2012. p. 1–6. Available from: https://doi.org/10.1049/cp.2012.0156

[12] Sahu TP, et al. Simulation and analysis of perturb and observe MPPT algorithm for PV array using Ćuk converter. 2014. Available from: https://api.semanticscholar.org/CorpusID:18269765

[13] Nema P, Nema RK, Rangnekar S. A current and future state of art development of hybrid energy system using wind and PV-solar: A review. *Renewable and Sustainable Energy Reviews*. 2009;13(8):2096–2103. Available from: https://doi.org/10.1016/j.rser.2008.10.006

[14] Zahraee SM, Assadi MK, Saidur R. Application of Artificial Intelligence Methods for Hybrid Energy System Optimization. *Renewable and sustainable energy reviews*. 2016 Dec 1;66:617-630. Available from: https://doi.org/10.1016/j.rser.2016.08.028

[15] Gupta A, Saini RP, Sharma MP. Modelling of hybrid energy system—Part I: Problem formulation and model development. *Renewable Energy*. 2011;36(2):459–465. Available from: https://doi.org/10.1016/j.renene.2010.06.035

[16] Gupta A, Saini RP, Sharma MP. Modelling of hybrid energy system—Part II: Combined dispatch strategies and solution algorithm. *Renewable Energy*. 2011;36(2):466–473. Available from: https://doi.org/10.1016/j.renene.2009.04.035

[17] Manwell JF. Hybrid energy systems. *Encyclopedia of energy*. 2004 Jan 1;3(2004):215-29. Available from: https://d1wqtxts1xzle7.cloudfront.net/103722425/hybrid_systems_review-libre.pdf

[18] Oyinna B, David LE, Okedu KE, Diemuodeke OE, Kalam A, Colak I. SMS based reservoir condition monitoring sensor system for pumped hydro storage in mini-grids. *Measurement: Sensors*. 2024 Jun 1;33:101242. Available from: https://doi.org/10.1016/j.measen.2024.101242

[19] Krishna VM, Duvvuri SS, Sobhan PV, Yadlapati K, Sandeep V, Narendra BK. Experimental study on excitation phenomena of renewable energy source driven induction generator for isolated rural community loads. *Results in Engineering*. 2024 Mar 1;21:101761. Available from: https://doi.org/10.1016/j.rineng.2024.101761